Title	BNおよびAlTiO高誘電率ゲート絶縁体を用いたAlGaN/GaN金属-絶縁体-半導体ヘテロ接合電界効果トランジスタ
Author(s)	Nguyen, Quy Tuan
Citation	
Issue Date	2014-09
Type	Thesis or Dissertation
Text version	ETD
URL	http://hdl.handle.net/10119/12305
Rights	
Description	Supervisor:鈴木　寿一, マテリアルサイエンス研究科, 博士

AlGaN/GaN metal-insulator-semiconductor heterojunction field-effect transistors using BN and AlTiO high-k gate insulators

Suzuki laboratory, s1040204 Nguyen Quy Tuan

1 Introduction

GaN-based metal-insulator-semiconductor heterojunction field-effect transistors (MIS-HFETs) have been investigated owing to the merits of gate leakage reduction and passivation to suppress the current collapse. Gate insulators, such as Al_2O_3, HfO_2, TiO_2, or AlN, have been studied. Further developments of the MIS-HFETs using novel gate insulators suitable according to applications are important. A desired gate insulator should have:

- a wide energy gap E_g and a high breakdown field F_{br} for high-voltage operations,
- a high dielectric constant k for high transconductance, and
- a high thermal conductivity κ for good heat release suitable for high-power operations.

In particular, boron nitride (BN) exhibits a high F_{br}, high k, and very high κ [1, 2]. On the other hand, aluminum titanium oxide (AlTiO: an alloy of very high-k TiO_2 and wide-E_g Al_2O_3 [3]), which has intermediate properties between TiO_2 and Al_2O_3, is important to balance k and E_g [4, 5]. Therefore, BN and AlTiO are promising gate insulators for the MIS-HFETs.

In this work, we characterize physical properties of BN thin films obtained by RF magnetron sputtering and AlTiO thin films obtained by atomic layer deposition (ALD) for several Al compositions. Using such films, we fabricate BN/AlGaN/GaN MIS-HFETs (BN MIS-HFETs) and AlTiO/AlGaN/GaN MIS-HFETs (AlTiO MIS-HFETs). Then, we investigate their temperature-dependent characteristics; analyze electron transport properties for channel conduction and gate leakage, and estimate BN/AlGaN and AlTiO/AlGaN interface state densities.

2 BN thin films and BN/AlGaN/GaN MIS-HFETs

We characterized physical properties of amorphous BN thin films obtained by RF magnetron sputtering, which have $E_g \sim 5.7$ eV, $F_{br} \sim 5.5$ MV/cm, and $k \sim 7$. Using the BN films, we fabricated BN MIS-HFETs, which exhibit high maximum drain current I_D and no negative conductance, as shown in Fig. 1(a), suggesting good thermal release properties owing to the excellent κ of BN. We obtain very low gate leakage I_G, as shown in Fig. 1(b), indicating good insulating properties of BN. In addition, transconductance g_m shows a slightly high peak, but rapidly decreases for forward biases, indicating a weak gate controllability, suggesting high-density BN/AlGaN interface states near the conduction band.

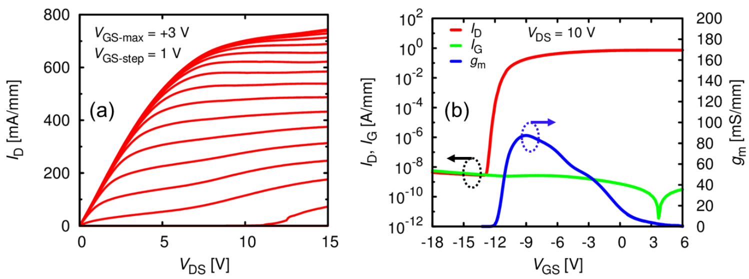

Figure 1: (a) Output characteristics and (b) transfer characteristics of BN MIS-HFETs at room temperature.

We investigated temperature-dependent channel conduction of the BN MIS-HFETs, where I_D decreases with increase in temperature. In the linear region, the decrease in I_D is attributed to decrease in the electron mobility, while the sheet electron concentration is constant. In the saturation region, the decreased I_D is proportional to the average electron velocity, whose temperature dependence is in-between those of the low- and high-field velocities, as shown by Monte-Carlo simulation [6] and indicated by experiments [7].

In order to elucidate temperature-dependent gate leakage of the BN MIS-HFETs, we carried out a fitting for two-terminal (drain open) gate-source leakage current I_{GS}, shown in Fig. 2(a), using

$$I_{GS}(V_{GS}, T) = I_0(V_{GS}) \exp\Big[-\frac{E_a(V_{GS})}{k_B T}\Big] + I_1(V_{GS}), \tag{1}$$

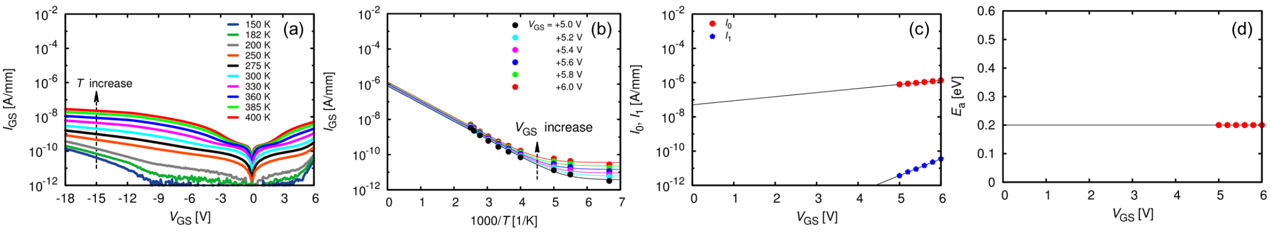

Figure 2: (a) Two-terminal (drain open) gate-source leakage current I_{GS} of the BN/AlGaN/GaN MIS-HFETs as functions of gate-source voltage V_{GS} for several temperatures T. (b) Experimental data is well fitted at large V_{GS}. (c) Prefactors I_0 and I_1, and (d) activation energy E_{a} as functions of V_{GS}.

with Boltzmann constant k_{B}, temperature T, activation energy E_{a}, prefactors I_0 and I_1, and gate-source voltage V_{GS}, where the first term is temperature-dependent and the second term is temperature-independent. We obtained good fittings, as shown in Fig. 2 (b). As a result, we observe $I_0(V_{\mathrm{GS}})$ and $I_1(V_{\mathrm{GS}})$ exponentially increase, as shown in Fig. 2(c), while $E_{\mathrm{a}}(V_{\mathrm{GS}})$ is almost constant, as shown in Fig. 2(d), with increase in V_{GS} at large forward biases. These indicate that the temperature-dependent term does not obey Poole-Frenkel (PF) mechanism. In order to explain the behaviors, we propose a mechanism with temperature-independent tunneling, dominant at low temperatures, and temperature-enhanced tunneling, dominant at high temperatures, as depicted in Fig. 3(a). By considering an equivalent circuit for DC limit, as shown in Fig. 3(b) [8], we estimated the BN/AlGaN interface state density, which is $\gg 10^{12}$ cm^{-2}eV^{-1}. High-density BN/AlGaN interface states lead to the weak gate controllability for the BN MIS-HFETs.

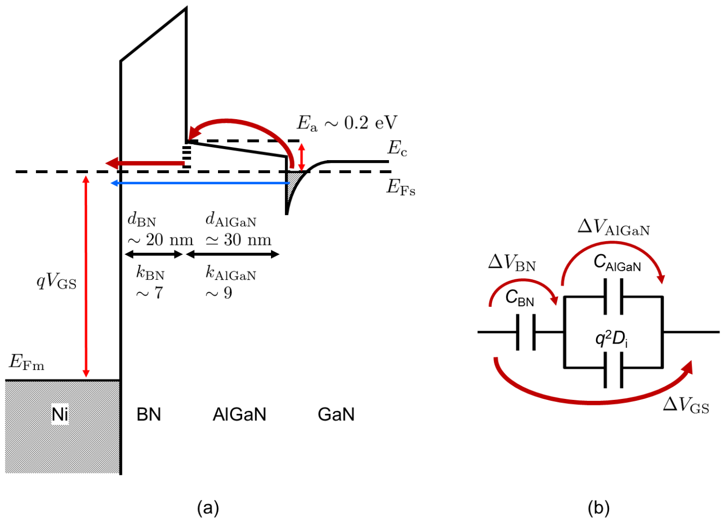

Figure 3: (a) Conduction band diagram of Ni/BN/AlGaN/GaN for a mechanism with temperature-independent tunneling and temperature-enhanced tunneling. (b) The equivalent circuit for the DC limit with BN capacitance C_{BN}, AlGaN capacitance C_{AlGaN}, and BN/AlGaN interface state density D_{i}.

3 AlTiO thin films and AlTiO/AlGaN/GaN MIS-HFETs

We characterized physical properties of $\mathrm{Al}_x\mathrm{Ti}_y\mathrm{O}$ thin films obtained by ALD, for several Al compositions $x/(x+y)$. We observe increasing E_{g} and F_{br}, and decreasing k with increase in the Al composition [9]. Considering the trade-off between k and F_{br}, we applied $\mathrm{Al}_x\mathrm{Ti}_y\mathrm{O}$ with $x : y = 0.73 : 0.27$, where $E_{\mathrm{g}} \sim 6$ eV, $F_{\mathrm{br}} \sim 6.5$ MV/cm, and $k \sim 24$, to fabrication of AlTiO MIS-HFETs. In comparison with $\mathrm{Al_2O_3}$/AlGaN/GaN MIS-HFETs, at room temperature, the AlTiO MIS-HFETs exhibit a higher maximum I_{D}, as shown in Fig. 4(a) and (b), a higher peak and better linearity of g_{m}, and a shallower threshold voltage, but a higher I_{G} (still very low), as shown in Fig. 4(c) and (d), suggesting that AlTiO is more favorable than $\mathrm{Al_2O_3}$ for applications to AlGaN/GaN MIS-HFETs. For the AlTiO MIS-HFETs, we observe a bump in I_{G} for high drain-source voltages V_{DS} and high I_{D}, indicating increase in channel temperature due to self-heating effects at high-power consumption. This suggests low-κ AlTiO due to random effects in alloy materials [10].

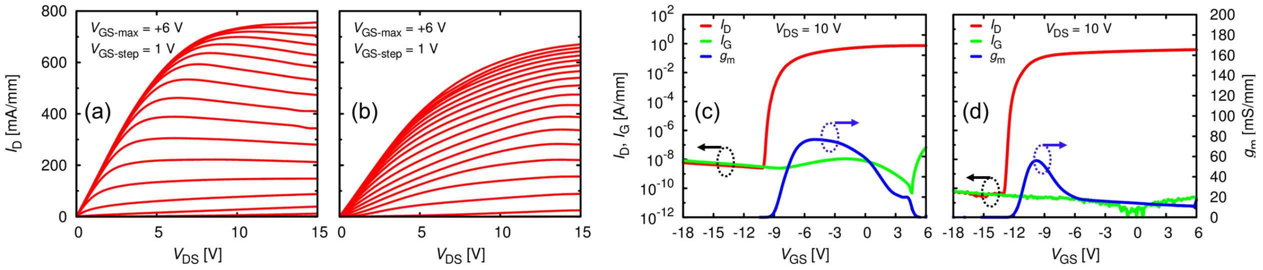

Figure 4: (a) and (b) Output characteristics, (c) and (d) transfer characteristics of AlTiO MIS-HFETs and Al_2O_3 MIS-HFETs, respectively.

We investigated temperature-dependent channel conduction of the AlTiO MIS-HFETs, where I_{D} decreases with increase in temperature. The behavior is similar to that of the BN MIS-HFETs. In the linear region, the decrease in I_{D} is mainly due to decrease in the electron mobility, while the contact resistance and the sheet electron concentration are almost constant. In the saturation region, the decreased I_{D} is proportional to the average electron velocity, whose temperature dependence is in-between those of the low- and high-field velocities.

In addition, we investigated temperature-dependent gate leakage for the AlTiO MIS-FETs by fitting two-terminal (drain open) gate-source leakage current I_{GS}, shown in Fig. 5(a), using Eq. (1). We obtained good fittings, as shown in Fig. 5(b). As a result, we observe temperature-independent term $I_1(V_{\mathrm{GS}})$ exponentially increases with increase in V_{GS}, as shown in the inset of Fig. 5(c), suggesting tunneling current through AlGaN and AlTiO barriers. In addition, for temperature-dependent term, we find that $I_0(V_{\mathrm{GS}})$ is a linear function of V_{GS}, or proportional to $(V_{\mathrm{GS}} - V_0)$ with $V_0 \simeq 2.9$ V, as shown in Fig. 5(c); and $E_{\mathrm{a}}(V_{\mathrm{GS}})$ is a linear function of $\sqrt{V_{\mathrm{GS}} - V_0}$, as shown in Fig. 5(d). The behaviors can be explained by the PF mechanism, described by [11]

$$I_{\mathrm{PF}}(F,T) \propto F \exp\left[-\frac{1}{k_{\mathrm{B}}T}\left(\phi - \sqrt{\frac{q^3 F}{\pi \varepsilon_0 k}}\right)\right], \tag{2}$$

with electron charge q, vacuum dielectric constant ε_0, electric field F in AlTiO, and trap depth $\phi \sim 0.41$ eV. The temperature-independent tunneling current, dominant at low temperatures, and PF current, dominant at high temperatures, are depicted in Fig. 6(a). By considering an equivalent circuit for DC limit, shown in Fig. 6(b) [8], we estimated AlTiO/AlGaN interface state density, which is $\sim 2 \times 10^{12}$ cm^{-2}eV^{-1}. Low-density AlTiO/AlGaN interface states lead to the strong gate controllability for the AlTiO MIS-HFETs.

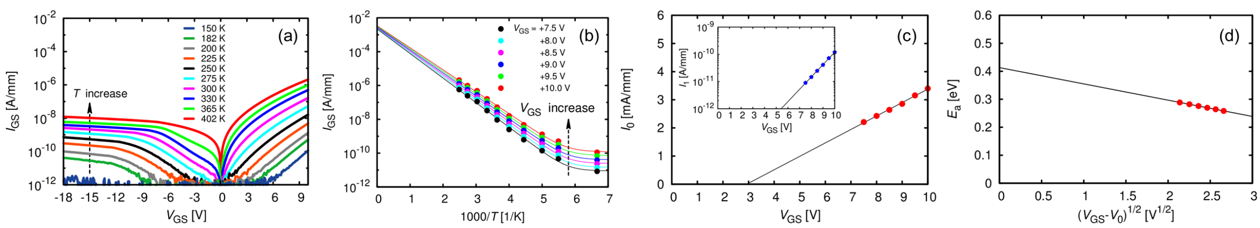

Figure 5: (a) Two-terminal (drain open) gate-source leakage current I_{GS} of the AlTiO/AlGaN/GaN MIS-HFETs as functions of gate-source voltage V_{GS} for several temperatures T. (b) Experimental data is well fitted at large V_{GS}. (c) Prefactor I_0 as a linear function of gate-source voltage V_{GS}, or proportional to $(V_{\mathrm{GS}} - V_0)$ with $V_0 \simeq 2.9$ V. The inset shows I_1 as an exponential function of V_{GS}. (d) Activation energy E_{a} as a function of $\sqrt{V_{\mathrm{GS}} - V_0}$.

4 Conclusions

We characterized physical properties of sputtering-deposited BN thin films and ALD AlTiO thin films for several Al compositions. Using such films, we fabricated BN MIS-HFETs and AlTiO MIS-HFETs. We investigated their temperature-dependent characteristics; analyzed electron transport properties for channel conduction and gate leakage, and estimated BN/AlGaN and AlTiO/AlGaN interface state densities.

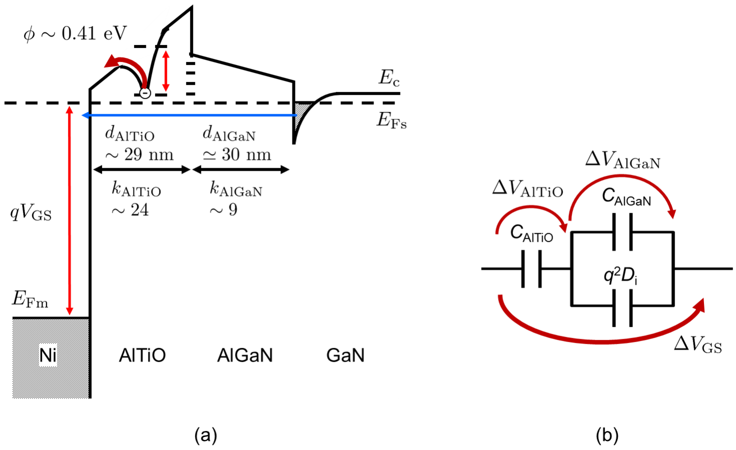

Figure 6: (a) Conduction band diagram of Ni/AlTiO/AlGaN/GaN with the temperature-independent tunneling and Poole-Frenkel currents. (b) The equivalent circuit for the DC limit with AlTiO capacitance C_{AlTiO}, AlGaN capacitance C_{AlGaN}, and AlTiO/AlGaN interface state density D_i.

References

[1] S. N. Mohammad, Solid-State Electron. **46**, 203 (2002).
[2] S. Adachi, *Properties of Group-IV, III-V and II-VI Semiconductors* (Wiley, England, 2005).
[3] J. Robertson, Rep. Prog. Phys. **69**, 327 (2006).
[4] C. Mahata, S. Mallik, T. Das, C. K. Maiti, G. K. Dalapati, C. C. Tan, C. K. Chia, H. Gao, M. K. Kumar, S. Y. Chiam, et al., Appl. Phys. Lett. **100**, 062905 (2012).
[5] E. Miranda, J. Suñé, T. Das, C. Mahata, and C. K. Maiti, J. Appl. Phys. **112**, 064113 (2012).
[6] U. V. Bhapkar and M. S. Shur, J. Appl. Phys. **82**, 1649 (1997).
[7] T. Tamura, J. Kotani, S. Kasai, and T. Hashizume, Appl. Phys. Express **1**, 023001 (2008).
[8] E. H. Nicollian and J. R. Brews, *MOS Physics and Technology* (John Wiley & Sons, New Jersey, 2003).
[9] T. Ui, M. Kudo, and T. Suzuki, Phys. Status Solidi C **10**, 1417 (2013).
[10] P. D. Maycock, Solid-State Electron. **10**, 161 (1967).
[11] J. Frenkel, Phys. Rev. **54**, 647 (1938).

Table of contents

1. Introduction 1
2. Fabrication process methods for AlGaN/GaN MIS-HFETs 20
3. BN thin films and BN/AlGaN/GaN MIS-HFETs 33
4. AlTiO thin films and AlTiO/AlGaN/GaN MIS-HFETs 58
5. Conclusions and future works 83
Appendix 86
References 92
List of publications 97

Refereed Journals

1. Tuan Quy Nguyen, Hong-An Shih, Masahiro Kudo, and Toshi-kazu Suzuki, "Fabrication and characterization of BN/AlGaN/GaN metal-insulator-semiconductor heterojunction field-effect transistors with sputtering-deposited BN gate dielectric", Physica Status Solidi C **10**, 1401 (2013).

2. Son Phuong Le, Tuan Quy Nguyen, Hong-An Shih, Masahiro Kudo, and Toshi-kazu Suzuki, "Low-frequency noise in AlN/AlGaN/GaN metal-insulator-semiconductor devices: a comparison with Schottky devices", Journal of Applied Physics, *in press*.

Keywords: AlGaN/GaN, MIS-HFET, BN, AlTiO, channel conduction, gate leakage, interface state